

## STATE OF THE ART AND DEVELOPMENT TRENDS OF NOVEL NANOSTRUCTURED ELASTOMAGNETIC COMPOSITES

L. Lanotte<sup>a\*</sup>, G. Ausanio<sup>a,b</sup>, C. Hison<sup>a,b</sup>, V. Iannotti<sup>a</sup>, C. Luponio<sup>a</sup>, C. Luponio Jr.<sup>b</sup>

<sup>a</sup>Istituto Nazionale per la Fisica della Materia (CNR) – UdR Na, Dip. di Scienze Fisiche,  
Università “Federico II”, P.le V. Tecchio 80, 80125 Napoli, Italy

<sup>b</sup>Dip. di Ingegneria dei Materiali e della Produzione, Università “Federico II”,  
P.le V. Tecchio 80, 80125 Napoli, Italy

The coupling between elastic and magnetic properties of composite materials made of magnetic particles uniformly dispersed into an elastic matrix was revised. The influence of particles content and size was considered. A unified simple model of the direct and inverse elastomagnetic effect was furnished explaining the experimental results in different experimental conditions. Some applications of elastomagnetic materials in both sensors and actuators are reported and their potentiality is discussed. The correlation between strain and electric conduction in this kind of materials is also presented and the first experimental results on this topic are reported.

(Received April 26, 2004; accepted June 3, 2004)

*Keywords:* Novel heterogeneous composites, Strain-magnetisation coupling,  
Strain-electric conductivity coupling.

### 1. Introduction

In the last years an increasing interest for composite materials made of magnetic particles inside a polymer or elastomer matrix can be noticed. Several different materials were tested: magnetoelastic composite with the filling particles made of magnetostrictive, hard or soft ferromagnetic material [1,2]; magnetorheological elastomers for application in airplane and car industries as actuators or anti-friction components [3]; heat-shrinkable elastic ferromagnets with variable magnetic and conductive properties [4].

This paper deals with a similar kind of material focusing on the theoretical and experimental correlation of the material elasticity with its magnetic behaviour and electric conduction. In particular we analyse the elastomagnetic and elastoresistive materials.

A composite of particles uniformly dispersed inside the matrix material is an elastomagnet if all the following requests are fulfilled: a) the particles have an asymmetric shape, preferably with a main anisotropy axis; b) the particles are soft ferromagnetic or small permanent magnets; c) the composite has an elastic behaviour, due to the matrix properties, up to a relative deformation of  $10^{-1}$ . In these conditions a strong coupling acts between magnetisation axis and the main shape anisotropy axis of the particles. Therefore a change of the magnetising field along an axis different from the easy magnetisation one (which is the permanent magnetisation axis when the filling particles are permanently magnetised) gives a rotation of the particles due to the mechanical torque, in order to align the magnetic moments with the applied field [5] (Fig. 1). The rotation may depend more or less on the elastic torque reaction of the matrix. When the torsional elastic coefficient,  $K$ , is less than 1 Nm, a local rotation of each particle of about  $10^{-2}$  rad can be produced [5]. The macroscopic effect of these local rotations can be a deformation of the whole material. This effect occurs by a mechanism independent on the intrinsic magnetostriction and it is named “direct elastomagnetic effect”. The inverse effect [6] consists in the change of magnetisation axis due to a deformation of the elastic material. As an example, an elongation of the elastomagnetic material

---

\* Corresponding author: lanotte@na.infn.it

produces a rotation of each particle and a consequent rotation of its magnetic moment because it is strongly coupled with the particles geometry (Fig. 2). This also gives a variation of the magnetisation component along the elongation axis ( $\Delta m_z = m'_z - m_z$  - Fig. 2). In conclusion the inverse elastomagnetic effect can be used to have a strain sensor detecting deformation by means of the induced magnetisation changes at constant temperature and magnetising field.

In the following we will examine: the magnetic properties of an elastomagnetic composite, a possible simple model of the elastomagnetic effect and its potential applications as sensor or actuator.

Elastoresistive materials are composites with the following characteristics: a) conductive particles uniformly dispersed into an elastic matrix; b) the particle content is near the percolation threshold so that a small decrease of sample volume can give an abrupt increase of the conductivity.

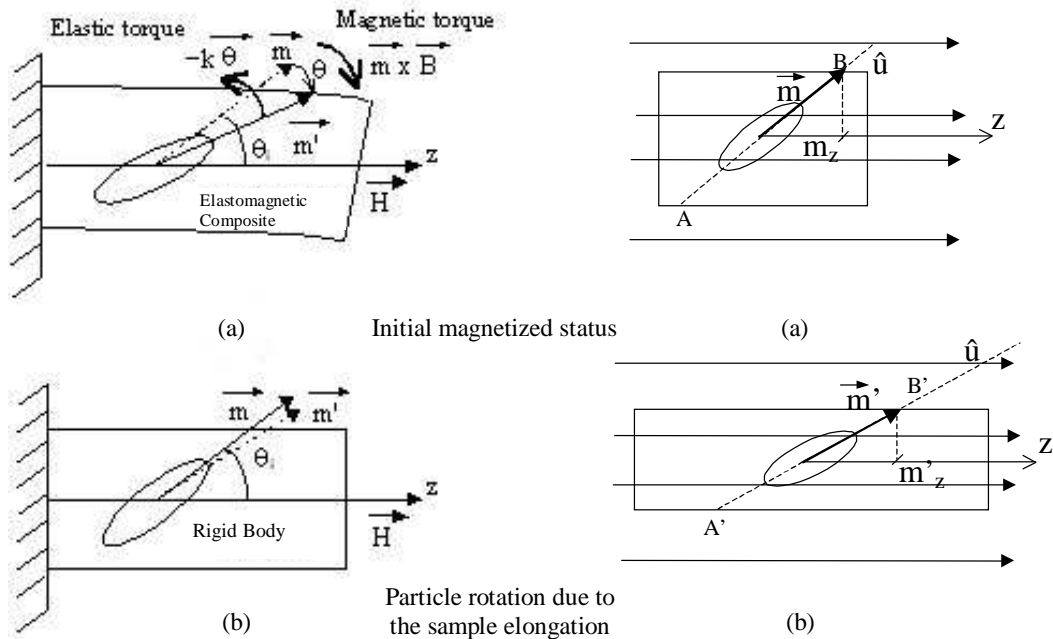


Fig. 1. Magnetising field effect on a magnetic particle inside an elastomagnetic bar matrix (a) compared to a rigid bar matrix (b).  $m$  = particle magnetic moment before  $H$  application;  $m'$  = particle magnetic moment after  $H$  application.

Fig. 2. Elongation strain effect on a magnetised particle (inside a composite material) with the magnetic moment strongly coupled to the shape anisotropy axis,  $u$ .

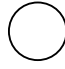


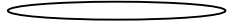

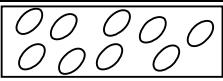
In these composites any deformation related to a change of the total volume gives a variation of the average distance among the particles. This distance change can produce the passage, in a verse or the other, between a status of isolated particles, for which only the tunnelling of the electrons can occur as conduction mechanism, to a status of particles in reciprocal contact, so that a great change of electric conductivity is governed by deformation. In ideal condition the effect should be reversible due to the material elasticity: in the following we approach deeply this argument and we will report some first experimental results.

## 2. Material preparation and experimental

The magnetic particles used may be commercial or produced in laboratory by any of the techniques generally adopted to have well-defined shape and size (physical deposition, chemical reaction, etc). After the particles selection on the basis of the desired properties (magnetic, conductive, geometric), the composite production occurs in three main steps: 1. mechanical dispersion of the particles inside the chosen elastic matrix when the latter is in liquid state; 2. solidification of the matrix without particles migration to form clusters but, if useful, with their

preorientation by application of a uniform magnetising field (about 0.5 T) in the desired direction; 3. permanent magnetisation of the particles by means of an intense magnetic field ( $\geq 2$ T) after the complete solidification of the matrix. The 3<sup>rd</sup> step is necessary only when the correlation between particle geometry and its magnetic moment axis is obtained not by the shape anisotropy but by permanent magnetisation (this is also the method to have the strongest coupling).

Table 1. Scheme of the possible geometry of the filling particles and resulting material.

Particles composition	Ni, Co, Fe, Fe <sub>2</sub> O <sub>3</sub> , SmCo	
Particles Size	 1-5 $\mu\text{m}$	 10-20 nm
Particles Shape	 Ellipsoidal	 Lenticular
Whole sample	 Random	 Preferential Preorientation
Initial Magnetic State	Demagnetised	Permanently Magnetised

The particles volume fraction may be chosen low ( $< 10\%$ ) in order to have no-interacting particles from both geometric and magnetic point of view, or high (up to 30%) if it is necessary to increase the elastomagnetic effect contribution. The volume fraction of 30% must not be overcome since the particles should rotate without being obstructed one by the other. The same procedure can be used for both elastomagnetic and elastoresistive materials.

The structural characterisation of the composite was performed by Atomic Force Microscopy, magnetic behaviour was tested by Vibrating Sample Magnetometry (VSM), deformation control was obtained by mechanical micro-devices and visualised by High Resolution Optical Microscopy. In Table I the scheme of the possible geometry of the magnetic particles and the final composite configuration are reported.

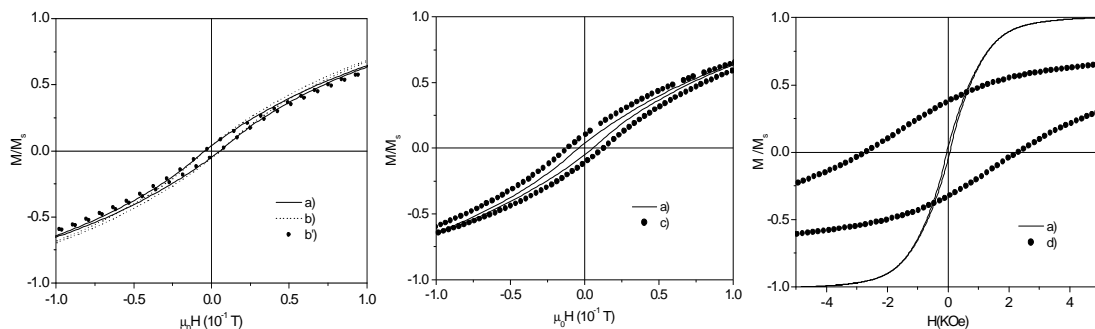


Fig. 3. Magnetisation cycles obtained by VSM at 250 K for elastomagnetic samples made of silicone matrix and magnetic particles: a) soft Ni particles of ellipsoidal shape, 5  $\mu\text{m}$  in average size on the major axis, randomly distributed; b) the same particles of case a) but after induced preferred orientation of the major axis along H field axis; b') the same particles of case a) but with a preferential orientation of the major axis orthogonal to H field axis; c) the same particles of case a) but with an average size on the major axis of about 40 nm; d) hard Sm<sub>2</sub>Co<sub>7</sub> magnetic particles of ellipsoidal shape, 5  $\mu\text{m}$  in average size on the major axis, randomly distributed.

### 3. Magnetic behaviour of an elastomagnet

The magnetic response of a composite of magnetic particles inside a non-magnetic elastic matrix depends strongly on the particles orientation because if it is random, any axis is equivalent for magnetisation, while if particles are pre-oriented with their easy magnetisation axes all parallel,

the magnetisation along this axis is easier than along the other ones. This fact can be seen in Fig. 3 by comparing case a, b and b'. On the other hand, magnetisation cycle depends on particles size. Going from micro to nano-particles, coercivity, saturation field, hysteretic area and remanent magnetisation increase - cycles a and c in Fig. 3.

All these may be explained by considering that more the particles dimension is decreasing, at fixed content of the magnetic component inside the elastomagnet composite, more each particle can be considered a single domain: it is more difficult to magnetise it, but saturation magnetisation tends to be maintained. On the other hand, the magnetisation cycle are very different when the particle material changes from a soft to a hard ferromagnet with tendency to permanent magnetisation (compare the cycles a and d in Fig. 3). For the optimum elastomagnetic performance it is useful to have nano-particles and permanent magnetisation, since the first request permits to increase particles content without inducing magnetic and mechanical interactions among them, and the second characteristic gives the strongest coupling between particle physical rotation and magnetic moment rotation.

#### 4. Elastomagnetic effect modelling

Consider a single asymmetric particle with a high coupling between the geometric and magnetic moment axes due to a strong shape anisotropy or an induced permanent magnetisation.

When a magnetising field  $\mathbf{H}$  is applied along z-axis a magnetic torque is produced - Fig. 1 (a) -  $\mathbf{M}_m = \mathbf{m} \times \mu_0 \mathbf{H}$ , where  $\mu_0$  is the vacuum permeability. The following model holds in the hypothesis that the magnetic torque is the prominent H effect. This takes place for H values that do not overcome the coercive field of the particles (that is about  $10^5$  A/m when permanent magnetic material is used). Since the matrix containing the particle is an elastic one ( $K$ = torque elastic constant), an elastic moment also acts:  $\mathbf{M}_e = -K \boldsymbol{\theta}$ , where  $\boldsymbol{\theta}$  is the effective particle rotation.

The equilibrium condition requires that:

$$m\mu_0 H_z \sin(\theta_i + \theta) = -K\theta \quad (1)$$

where  $\theta_i$  is the initial angle between  $\mathbf{m}$  and  $\mathbf{H}$  - see Fig. 1 (a); the convention is  $\theta < 0$ ).

Taking into account that generally  $|\theta| < 10^{-2}$  rad, Eq. (1) is practically equivalent to

$$m\mu_0 H_z \sin \theta_i \cong -K\theta \quad (2)$$

In order to have the behaviour of the whole elastomagnetic sample it is consistent to consider the average magnetic moment of the sample  $m^* = M_r \tau V\%$  (where  $M_r$  is the remanent magnetisation intensity of the particle,  $\tau$  is the total sample volume and  $V\%$  is the volume fraction of the magnetic particles inside the composite) instead of single particle moment. In order to evaluate the macroscopic practical effect Eq. (1) becomes:

$$\theta \cong \frac{-M_r V\% \tau \mu_0 H_z \sin \theta_i}{K} \quad (3)$$

Since the rotation of  $\mathbf{m}$  towards  $\mathbf{H}$  means an easier magnetisation along z-axis, from Eq. (3) it is clearly deduced that more the material is elastic (small  $K$ ), more the magnetisation is easy along the applied field axis. Moreover the effect is maximum if the particle magnetisation is maximum and it depends on the initial orientation of the particles magnetic moment.

Consider now also the presence of an external strain component  $\varepsilon_z$  along the same axis of  $\mathbf{H}$ . Following Ref. [7] it is easy to see that the rotation determined only by strain is:

$$\theta'_\varepsilon = \varepsilon_z \sin \theta_i \cos \theta_i \quad (4)$$

In the presence of both  $\varepsilon_z$  and  $\mathbf{H}$ , the Eq. (1) becomes:

$$m\mu_0 H_z \sin(\theta_i + \theta) = K(\theta'_\varepsilon - \theta) \quad (5)$$

where the standard convention for  $\theta$  sign is applied.

From Eq. (5), considering  $m^*$  instead of  $m$ , and  $|\theta| < 10^{-2}$  rad, one finds:

$$\theta = \frac{-K\varepsilon_z \sin \theta_i \cos \theta_i - m^* \mu_0 H_z \sin \theta_i}{K + m^* \mu_0 H_z \cos \theta_i} \quad (6)$$

This is the constitutive equation of elastomagnetism, relating average particle rotation  $\theta$  to externally applied uniaxial strain  $\varepsilon_z$  and field  $H_z$ . It takes into account the initial preorientation of the magnetic moments  $\theta_i$  and the elastic (K) and magnetic ( $M_r$ ) properties of the composite material.

Eq. (6) can describe the effective rotation determined only by strain application, at constant field, as the difference between  $\theta$  value obtained at  $\varepsilon_z \neq 0$  and that at  $\varepsilon_z = 0$ . From this difference one obtains

$$\theta_\varepsilon = \frac{-K\varepsilon_z \sin \theta_i \cos \theta_i}{K + M_r \tau V \% \mu_0 H_z \cos \theta_i} \quad (7)$$

Note the coherence of the minus sign with the physical effect (Fig. 2): at constant positive denominator, when the relative deformation component  $\varepsilon$  is positive (elongation) the particles rotation  $\theta_\varepsilon$  is negative (in the clockwise direction) and vice versa.

The inverse elastomagnetic effect is described by Eq. (7). In effect, considering magnetisation vector parallel to  $\mathbf{m}$ , by projection on z-axis, one calculates the change of magnetisation component along  $\mathbf{H}$  axis,  $\Delta M_z$ , due to  $\varepsilon_z$  at constant H. It is easy to find [7]:

$$\Delta M_\varepsilon = -M_r V \% \theta_\varepsilon \sin \theta_i = \frac{K\varepsilon_z M_r V \% \sin^2 \theta_i \cos \theta_i}{K + M_r \tau V \% \mu_0 H_z \cos \theta_i} \quad (8)$$

On the other hand, Eq. (6) is able to describe also the direct elastomagnetic effect if the rotation  $\theta$  is evaluated as produced only by the applied magnetic field, namely at zero external deformation. The

obtained relation is

$$\theta_H = -\frac{M_r \tau V \% \mu_0 H_z \sin \theta_i}{K + M_r \tau V \% \mu_0 H_z \cos \theta_i} \quad (9)$$

where  $\theta_H$  is the local macroscopic average rotation determined only by  $H_z$  action. Also in this case it is verified the coherence of the signs with the physical actual effect (Fig. 1): if  $H_z > 0$  there is  $\theta_H < 0$  (clockwise rotation).

In the practical cases investigated in the next paragraph we will use Eqs. (8) and (9), verifying their validity in prototypes of devices using elastomagnetic material core.

## 5. Experimental results from first prototypes of elastomagnetic sensors and actuators

The elastomagnetic composite sample is constituted by four bars of silicone uniformly filled with 9% of  $\text{Sm}_2\text{Co}_7$  particles. In each bar was induced a permanent magnetisation so that all the particle magnetic moments are aligned at  $45^\circ$  with respect the longitudinal z-axis (Fig. 4).

In the opposite bars the magnetic moments orientation is symmetric with respect to z-axis, so that the macroscopic magnetisation has zero transverse component, while a total longitudinal magnetisation  $M_z = (\sum m/\tau) \sqrt{2}/2$ , due to the projection of each particle moment along z-axis, is permanently present. A similar composite sample can be the core of a sensor or an actuator.

A sensor device can be obtained as shown in Fig. 5 by fixing the extremities of the elastic magnet sample of Fig. 4 between two rigid plates attached on the deforming body to be monitored, so that the relative y axis deformation  $\varepsilon_z$ , on z-axis, is transduced by the elastomagnetic sample. A rigid coil, with z symmetry axis, is wound around this sample and it detects the induce electromotive force due to  $M_z$  change determined by the magnetic moments rotation as consequence of  $\varepsilon_z$ . Taking into account the used condition in the described prototype, we have:  $M_r = 0.6 \times 10^6$  A/m;  $V \% = 9\%$ ;  $H = 0$  A/m;  $K = 1$  Nm;  $\tau = 5 \times 10^{-6}$  m<sup>3</sup>. Therefore Eq. (8) gives:

$$\Delta M_z = M_r \varepsilon_z V \% \sin^2 \theta_i \cos \theta_i = C \varepsilon_z \quad (10)$$

where  $C \approx 1.9 \times 10^4$  A/m is the proportionality constant between the strain and the induced magnetisation change. On the other hand it is immediate to calculate the induced electromotive force as

$$V = -\frac{\partial(\mu_0 \Delta M_z N S)}{\partial t} = -C \mu_0 N S \frac{\partial \varepsilon_z}{\partial t} \quad (11)$$

where  $N$  is the number of coil turns and  $S$  is the sample cross section.

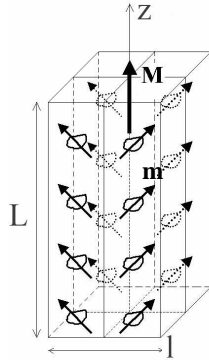


Fig. 4. View of the elastic magnet obtained by four elastomagnetic bars with permanent magnetic moment,  $m$ , of the  $\text{Sm}_2\text{Co}_7$  particles oriented at  $\pi/4$  with respect to the sample longitudinal axis, so that the macroscopic magnetization  $M$  has no transverse component but high longitudinal one.  $L=50$  mm,  $l = 10$  mm.

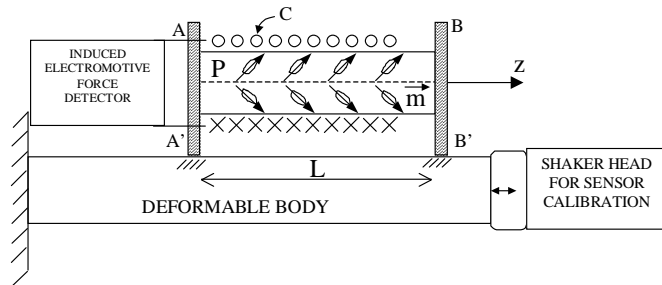


Fig. 5. Scheme of the elastomagnetic sensor able to measure relative longitudinal deformation along  $z$ -axis.  $P$  = elastomagnetic sample composed as in Fig 4 with orientation of particles moment  $m$  at  $\pi/4$  with respect to  $z$ -axis.  $AA'$  and  $BB'$  = rigid plates fixed on the deformable body in  $A'$  and  $B'$ , respectively;  $C$  = rigid coil fixed on the plate  $AA'$ .

Eq. (11) evidences the usefulness of the proposed sensor in the case of harmonic oscillations. In effect, when we are in this case,  $\varepsilon_z$  can be represented by the expression  $\varepsilon_z(t) = (\Delta L/L) \sin(2\pi\nu t + \phi)$  where  $\nu$  is the vibration frequency and  $L$  is the initial length of the monitored region. From Eq. (11) is deduced  $V(t)$  amplitude which is proportional to the oscillation amplitude:  $V_0 = C' \Delta L$  where  $C' = 2\pi\nu\mu_0 N S C/L$  and, in the used condition, its value is about  $7$  V/m ( $N=500$  and  $\nu=50$  Hz). In order to verify the model predictions, the vibration of the monitored body was simulated by means of a shaker working at  $50$  Hz and producing relative displacements from  $0.01$  mm up to  $2$  mm.

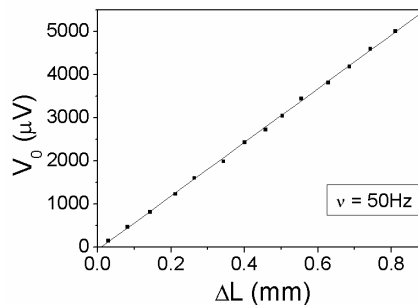


Fig. 6. Calibration curve of the elastomagnetic sensor for longitudinal vibration at  $\nu = 50$  Hz.  $V_0$  amplitude of the induced electromotive force as a function of the relative displacement,  $\Delta L$ , between the two monitored points  $A'$  and  $B'$ .

From the experimental results presented in Fig. 6 it is possible to confirm the linear behaviour of  $V_0$  versus  $\Delta L$  and to evaluate a proportionality constant very close to that deduced from the simple theoretical model.

Sensors similar to that here described can be used also for torsion or flexional deformation detection and generally good linear experimental curves ( $V_0$  versus deformation of the monitored component) were obtained from  $20$  up to  $150$  Hz, which is the useful range for mechanical vibrations study.

We will consider now the application of an elastomagnetic core for actuation purposes. A possible actuator configuration is shown in Fig. 7 where the elastomagnetic sample has the same structure shown in Fig. 4. When a magnetising field is applied by means of a coil on the elastic magnet, Eq. (9) is valid.

Moreover, since the device arrangement does not enable flexional deformation of the elastomagnetic core, the rotation  $\theta_H$  becomes a longitudinal relative deformation [8], following the equation

$$\varepsilon_{zH} \cong -\frac{\sqrt{2}}{2} \theta_H = \frac{\sqrt{2}}{2} \frac{M_r \tau \mu_0 H_z V\% \sin \theta_i}{K + M_r \tau \mu_0 H_z V\% \cos \theta_i} \cong \frac{1}{2} \frac{M_r \tau \mu_0 H_z V\%}{K} \quad (12)$$

where in the last term was taken into account that  $\sin \theta_i = \sqrt{2}/2$  and that the second term at denominator is much lower in comparison with the first one in the case of the used value for the experimental parameters (in effect  $\mu_0 H_z < 0.1$  T where  $H_z$  is the modulus of the applied field). A similar actuator can apply on an external body, which impedes its free deformation, a maximum force

$$F = ES\varepsilon_{zH} = \frac{1}{2} \frac{M_r \tau \mu_0 H_z V\% ES}{K} \quad (13)$$

where  $E$  is the Young Modulus of the elastomagnetic core. Therefore from Eq. (13) it is easy to conclude that in order to produce and transmit the highest force, at constant exciting field  $H_z$ , it is necessary to use the highest possible permanent magnetisation, volume fraction of magnetised particles, Young Modulus of the matrix material and section area of the sample orthogonal to the force (displacement) axis; at the same time the lowest possible torsion elastic constant of the silicone should be used. Obviously, fixed the other parameters,  $F$  value is proportional to  $H_z$ .

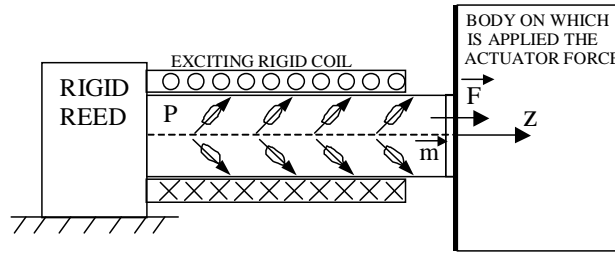


Fig. 7. Scheme of an elastomagnetic actuator. (P = composite sample as in Fig. 4).

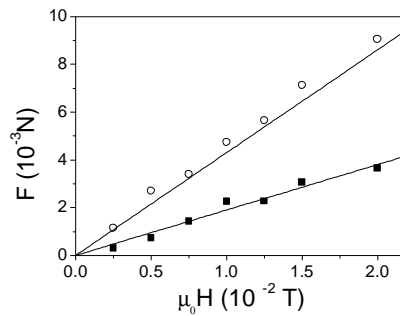


Fig. 8. Force produced by the elastomagnetic actuator versus the exciting field for two values of particles volume fraction:  $\blacksquare$   $V\% = 4\%$  and  $\circ$   $V\% = 9\%$ . The experimental points behave in agreement with the theoretical lines obtained from Eq. 13. One can see that the experimental points for  $V\% = 9\%$  are a little higher than the theoretical line; this is probably due the fact that when  $V\%$  increases the ratio  $E/K$  is higher than the one of Eq. 13 used to obtain the theoretical curve (referring to the pure silicone matrix).

In order to have an experimental test of these last predictions, a load cell was put on the free side of the extending sample and  $F$  as function of  $H_z$  was directly detected for different values of the particles content. In Fig. 8 are shown the obtained experimental curves. The value of the experimental parameters  $M_r$ ,  $S$ ,  $K$  and  $\tau$  are the same with those indicated for the sensor device previously examined, while it was determined that the used silicone has  $E = 3.1 \times 10^4$  Pa. It is possible to verify the linear behaviour and to measure an experimental proportionality constant between  $F$  and  $\mu_0 H_z$  which is very close to that evaluated from Eq. (13) (theoretical values 0.19 and 0.43 for  $V\%$  equal to 4% and 9%, respectively).

As a more general picture of the state of the art for the elastomagnetic material application, in Table II the potential performances obtainable in the best conditions by an elastomagnetic composite are compared with those of other competitive materials actually used for sensors or actuators of static or dynamic deformation. From Table II it is evident that the energy density for elastomagnetic bulk materials is not so good but the possible actuating strain is very high.

In conclusion one can affirm that the application of elastomagnetic composite may be competitive in the field of micro control or strain sensor devices, while in the actuators field it may be useful only in particular cases, as for example when a special shape of actuator is necessary or in tele-operated and biomedical components or also if high force production is required on a very great surface.

Table 2. Comparison between the actuation performances of the investigated elastomagnetic composite and two standard materials (Piezoelectric and Magnetostrictive) for actuators.

Actuator type	Max Strain (%)	Max Pressure (MPa)	Max Energy Density (J/cm <sup>3</sup> )	Max Efficiency (%)	Relative Speed (full cycle)
Elastomagnetic Bulk Silicone (SmCo Filler VF 30%)	1.4	1×10 <sup>-2</sup>	7×10 <sup>-5</sup>	>80%	Medium
Piezoelectric					
Ceramic (PZT)	0.2	110	0.10	>90	Fast
Polymer (PVDF)	0.1	4.8	0.0024	90	Fast
Magnetostrictive (Terfenol-D, Etrema Products)	0.2	70	0.025	60	Fast

## 6. Modulate electron conductivity in elasto-resistive materials

Consider now an elastic material (silicone) in which conductive particles (nickel) are uniformly dispersed. If  $d$  is the average particles size and the sample has cubic shape of side  $l$ , consider the sample divided into cubic cells of side  $d \ll l$  and that each cell may be occupied or not by a particle with the probability increasing with the particles content in the sample. The value of  $V\%$  which enables the possibility to have continuous particle chains going from one side of the sample to the other (namely giving direct conduction paths between opposite sample sides) is expected to be between  $1/8$  and  $1/4$ . This is easily deduced considering that if  $V\% < 1/8$  it is impossible to have one continuous line of particles in contact along the whole sample, connecting one side to the other; on the other hand, when  $V\%$  reaches the value  $1/4$ , at least one line of this kind is necessarily present. Therefore to investigate the conduction properties of this kind of material around the passage from non-conductive to conductive behaviour (through the percolation threshold), several samples, containing nickel particles ( $d \approx 5\mu\text{m}$ ) uniformly dispersed into the silicone matrix, were prepared with the particles volume fraction going from 12% to 25%. Their specific resistance  $\rho$  was evaluated using the apparatus shown in Fig. 9. This apparatus was predisposed to give also a volume contraction of the sample, which being effective only on the silicone matrix, induces an increment of the conductive particle volume fraction.

In Fig. 10 is presented the resistivity behaviour versus volume fraction of nickel particles in elastoelectric material. The obtained results verify that the chosen range of  $V\%$  is the right one to observe the transition from non-conductive to conductive status; moreover the percolation threshold can be experimentally individuated around  $V\% \approx 18\%$ .

When a uniaxial strain  $\epsilon = \Delta l/l$  is produced by means of a displacement  $\Delta l$  of the cursor in Fig. 9, since the cross section is constant, the volume sample contraction is just equal to  $\epsilon$ . The silicone density increases while the nickel particle density remains practically unchanged, due to the very high elasticity modulus of the last component with respect to the first one. As a consequence, the volume fraction of the nickel particles inside the sample changes from the initial value  $V\%$  to  $V\%^* = V\% / (1 - |\epsilon|)$ . If, as an example, the initial value of the nickel fraction is 18%, after a contraction of  $\epsilon = -16.7 \times 10^{-2}$  the nickel fraction is about 21%. Therefore, if conductivity is governed by nickel particle abundance, one expects that its change gives a new resistivity predicable from the data of Fig. 10. In the case of the last example, there is expected a variation in resistivity correspondent to the change from  $V\% = 18\%$  to 21%, with a total enormous decrease from  $10^{11} \Omega\text{cm}$  to  $10 \Omega\text{cm}$ .



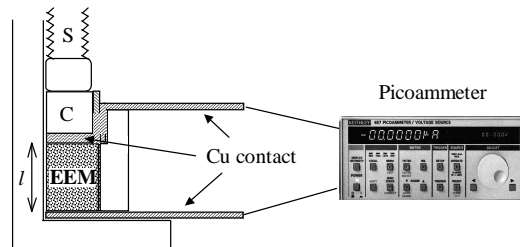


Fig. 9. Cross section view of the apparatus for resistivity measurement. (S = micrometric screw; C = cursor; EEM = elasto-electric material;  $l$  = sample length as produced).

Following the preceding consideration, a negligible effect of contraction is expected in the sample with low or high initial  $V\%$  value (15% or 24%), while the most considerable effect is expected around initial  $V\%$  value of 18%. In Fig. 11 the resistivity  $\rho$  behaviour, obtained by repeated measurements in elasto-resistive samples with different initial values of  $V\%$ , as a function of the applied  $\varepsilon$  is reported. The equivalent expected volume fraction of nickel particles, after contraction, is also indicated on the horizontal axis.

It can be verified that qualitatively, the expectations are valid, but  $\rho$  decrease in 18% sample is not so high as that of the ideal behaviour deducible from data of Fig. 10 and reported in Fig. 11.

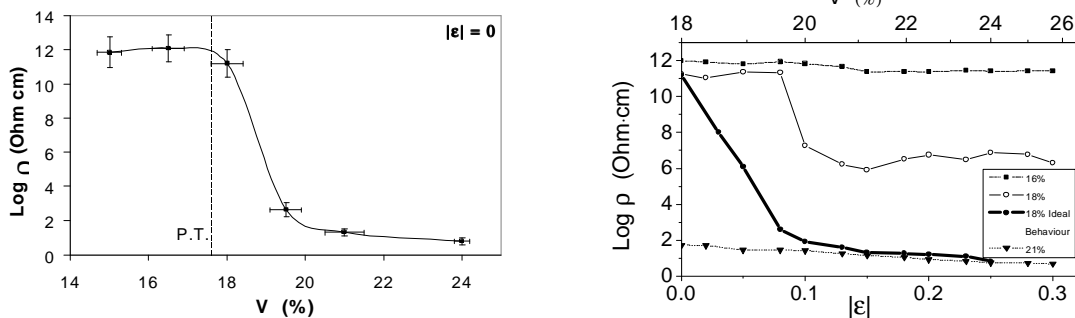


Fig. 10. Resistivity behaviour,  $\log \rho$ , versus volume fraction  $V\%$  of nickel particles in elastoelectric material. P.T. = Percolation Threshold.

Fig. 11. Log of resistivity,  $\rho$ , in composite material of nickel particles uniformly dispersed in silicone matrix as function of an uniaxial strain  $\varepsilon$  for different initial volume fraction of nickel,  $V\%$ . Bold line reports the expected  $\log \rho$  values in 18% sample if the effect of compressive uniaxial strain is considered equivalent to an increase of nickel volume fraction (data deduced from Fig. 10).

The experimental  $\Delta\rho/\Delta\varepsilon$  value, lower than the theoretically evaluated one, can be explained by taking into consideration that the silicone density increases at the same way of  $V\%*$ ; therefore the sample conductive properties change not only because particles percentage changes but also because the aggregating material is more dense and it has a lower conductivity. In other words a higher potential barrier should be preset among the particles, which increases with  $|\varepsilon|$  and it inhibits the electron passage from a particle to the other [9].

To reach giant  $\Delta\rho/\Delta\varepsilon$  values it is necessary further work and also to improve the material structure and engineering. However the modulation of the resistivity by means of strain in elasto-resistive composite is clearly demonstrated by the first reported experimental results. Naturally, the effect can be used also to measure strain, stress or pressure by means of the induced conductivity change, with application in novel and ductile load cells or strain gauges.

It is interesting to observe that the samples used in this last section are elasto-resistive ( $\varepsilon$  induces  $\rho$  change) but at the same time they are also elastomagnetic if the nickel particles have a high shape anisotropy. In perspective one can use acicular nickel particles so that by means of the direct elastomagnetic effect can be produced their rotation by an external magnetising field and, at the same time, a decrease of their reciprocal distance. In proper conditions this rotation can produce the contact among neighbour particles and a consequent change of resistivity. In other words it is

potentially possible to produce an elastomagnetic and elasto-resistive material in which a noteworthy variation of conductivity can be reversibly induced by the application of a magnetic field at room temperature, in a way completely independent from the standard magnetoresistance.

## 7. Conclusions

The behaviour of composite materials made of magnetic particles uniformly dispersed in an elastic matrix, under the action of an external magnetising field  $H$  and/or a strain  $\epsilon$ , was revised furnishing a unified simple model of the influence of  $H$  and/or  $\epsilon$ , in the hypothesis of a high coupling between particles body and their magnetic moment and that particles volume fraction are enough small to consider that they are not interacting from the magnetic and elastic point of view. Experimental validation of the simple theoretical description is reported in the case of  $\text{Sm}_2\text{Co}_7$  particles, permanently magnetised in a common preferential orientation. Moreover it is shown how some applications in sensors and actuators are already developed and a comparison with the devices operating with standard magnetostrictive or piezoelectric materials is given. In particular, due to the large strain potentially obtainable, the elastomagnetic composites appear very useful in deformation sensors, while their potentiality as actuator core results strictly related to specific cases in which not usual shape is necessary or large surface are to be controlled.

The study of conductive properties in composite of conductive particles uniformly dispersed in a non-conductive, elastic matrix was also approached in this paper. In the case of nickel particles inside silicone, it was shown how the volume fraction  $V\%$  of the conductive particles in as-prepared samples can be tailored in order to have a large resistivity range, from  $10^{11}$  to  $10 \Omega\text{cm}$  for  $V\%$  going from 15% to 24%; the percolation threshold was evidenced near 18%. In samples near this threshold condition, the possibility to obtain the elasto-resistive effect, namely a noteworthy change of resistivity produced by the strain, was demonstrated. To reach the effectiveness in practical application of this elasto-resistive effect a lot of work is necessary; in particular is necessary to obtain the proper artificial composite in which the direct effect of strain is only a change of particles density. However the perspective that are deducible by considering the actual possibility to build a material which is elastomagnetic and elasto-resistive at the same time (therefore magneto-resistive) are interesting for both fundamental knowledge and application development, justifying the intense increment of the studies in this field.

## Acknowledgement

This work was sponsored by the MURST FIRB project "Innovative Magnetic Materials Structured in Nanoscopic Scale". We are grateful to Dr. Carlo Campana for his contribution in measurements on elasto-resistive composite.

## References

- [1] T. A. Duenas, G. P. Carman, *J. Appl. Phys.* **87**, 4696 (2000).
- [2] S. Bednarek, *Chinese journal of Physics* **38**, 169 (2000).
- [3] M. Lokander, B. Stenberg, *Polymer Testing* **22**, 245 (2003).
- [4] S. Bednarek, *Mat. Sci. Eng. B* **77**, 120 (2000).
- [5] L. Lanotte, G. Ausanio, C. Hison, V. Iannotti, C. Luponio, *Sensors and Actuators A* **106**, 56 (2003).
- [6] L. Lanotte, G. Ausanio, V. Iannotti, G. Pepe, G. Carotenuto, P. Netti, L. Nicolais, *P. R.* **B63**, 054438 (2001).
- [7] L. Lanotte, G. Ausanio, V. Iannotti, C. Luponio Jr, *Appl. Phys A* **77**, 953 (2003).
- [8] V. Iannotti, C. Hison, L. Lanotte, G. Ausanio, C. Luponio, A. D'Agostino, R. Germano, *Proceeding ISEM2003*, 246 (2003).
- [9] R. Zallen, *The Physics of Amorphous Solids* ed. Wiley, N.Y. (1983) Chapter 5, pp. 223.